LASER INTERFEROMETER GRAVITATIONAL WAVE OBSERVATORY

– LIGO –

CALIFORNIA INSTITUTE OF TECHNOLOGY
MASSACHUSETTS INSTITUTE OF TECHNOLOGY

Document Type LIGO-T000123-00-R 11/7/00
Wavefront Sensing for the 40m LIGO Prototype
Brian Kappus, Alan Weinstein

Distribution of this draft:

This is an internal working note
Of the LIGO Project

California Institute of Technology
LIGO Project – MS 51-33
Pasadena, CA 91125
Phone (626)395-2129
Fax (626)304-9834
E-mail: info@ligo.caltech.edu

Massachusetts Institute of Technology
LIGO Project – MS 20B-145
Cambridge, MA 01239
Phone (617)253-4824
Fax (617)253-7014
E-mail: info@ligo.mit.edu

WWW: http://www.ligo.caltech.edu

Wavefront Sensing for the 40m LIGO Prototype

Brian Kappus
Mentor: Alan Weinstein

Abstract

The LIGO interferometers rely on suspended optics for their seismic isolation as well as to simulate a freely falling body above low frequencies. Yet allowing the mirrors to swing freely presents the problem of keeping the interferometer in lock. This entails keeping the mirrors aligned and cavity lengths adjusted to keep the beam resonant in the cavities. An alignment sensing scheme called "wavefront sensing" was developed by Daniel Sigg, Nergis Malvalvala, and others for the current LIGO I configuration, but has yet to be applied to the signal recycling scheme proposed for LIGO II. In this project, I used a Mathematica model designed by Daniel Sigg to generate an effectively diagonal wavefront sensing matrix for the 40m LIGO Prototype which includes a signal recycling mirror.

Introduction

As predicted by Einstein, when extremely large masses spiral into each other they release energy in the form of gravitational waves. These waves propagate through space at the speed of light and cause spatial disturbances. These disturbances give rise to length strains on the order of $\Delta L/L \sim 10^{-21}$.

Variants of a Michelson Interferometer have been proposed as detectors. They are ideal for detecting the quadrupolar strain caused by gravitational because of their sensitivity to differential arm length changes. Because gravitational wave strain causes displacement proportional to initial length, we can get a larger signal in a Michelson configuration by having longer arms. Yet, from an engineering standpoint, longer arms require larger vacuums and introduce more design problems. So, instead we can "fold" the arm by recycling the beam. In other words, we design the arm so that the beam bounces the length of the arm several times, thus amplifying the phase shift (and thus the signal) caused by a mirror movement.

The current proposed setup for the Laser Interferometric Gravitational Wave Observatory (LIGO) consists of a Michelson interferometer with Fabry-Perot cavities in each arm as well as a power recycling mirror between the input beam and the beam splitter and, in an advanced configuration, a signal recycling mirror at the dark port. The power recycling mirror reflects the light back into the interferometer which would otherwise just leak out of the system. This increases the power in the cavities and doesn't waste as much laser power. Increasing the power in the cavities decreases the effect of

shot noise on the strain sensitivity. The signal recycling mirror is able to amplify gravity wave signals in a particular frequency band by tuning the signal recycling cavity resonance just right.

Keeping the system in resonance is essential to maintaining the sensitivity of the detector. It is important to not only keep the arm lengths correctly in resonance, but in angular alignment as well. Misaligned mirrors cause higher order modes to appear in the cavity which reduces the amount of power circulating within the cavities because those modes are not resonant. It also reduces the GW signal, and introduces noise at the signal(dark) port. In other words, we need to hold the optical cavities on resonance for the lowest order mode by some locking scheme in order to maintain maximum sensitivity.

Methods

The typical alignment locking scheme is based on the Pound-Drever-Hall reflection locking technique. This technique was originally designed to keep a Fabry-Perot cavity in resonance. This method is particularly attractive since it uses light already circulating in the system to extract an error signal, which assures that the interferometer is aligned relative to the input beam.

The locking scheme senses length misalignment using set of phase modulated RF sidebands that are not resonant in the cavity. Since they are not resonant in the cavity, they simply reflect off as if they had hit a mirror. On the other hand, the carrier is very sensitive (in phase) to the movement of both mirrors. If we look at the beat frequency

between the carrier and the sidebands (demodulation) we can tell which direction in phase the carrier has moved if a mirror is moved. In other words, the sidebands serve as a constant phase reference with which to beat the carrier on in order to determine any movement.

The goal of my project was not to sense length changes, however, but rather angular misalignment. The technique is very similar to the length locking scheme described above, with some slight changes. The key to the angular alignment technique is to study the transverse profile of the beam in the resonant cavity. For a perfectly aligned cavity, the transverse modes look approximately like those given in Fig1. The number beyond TEM (transverse electromagnetic mode) denotes the order of the hermite polynomial with which that dimension is multiplied.

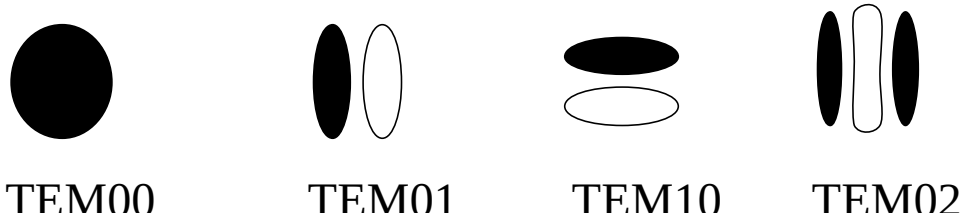

Fig 1. Transverse profiles of TEM modes

The angular alignment scheme is built around the concept that if one of the mirrors in the cavity becomes misaligned, the lowest order TEM_{00} mode of any frequency resonant in the cavity becomes coupled with higher order modes (this is shown in Fig. 2). On the other hand, since the sidebands are not resonant in the cavity, they are not affected. Where TEM_{00} modes are symmetric about the beam center, the higher order modes are not. By using a split photodiode, one that takes the difference between the

signal on each half of the photodiode, we can produce signal only in the presence of the TEM_{01} mode and not receive any false signal due to fluctuations in the TEM_{00} mode.

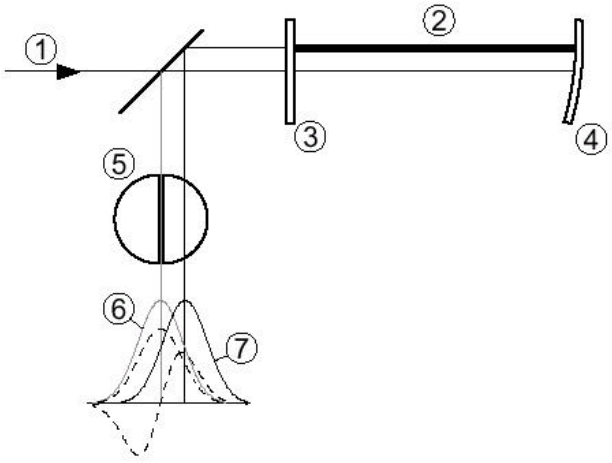

Fig 2. Transverse profile of a misaligned cavity

So we can demodulate at the same frequency that we did for the length sensing, but only be sensitive to angular misalignment. We can distinguish the misalignment signals of the input mirror as opposed to the end mirror by looking at the Guoy phase of the TEM_{01} modes. The Gouy phase is the additional phase advance acquired by the phase front of a hermite gaussian beam beyond that from a planar wave. This additional phase shift is acquired as it propagates, and is given in equation 1.

$$\text{Phi}(z) = (n+m+1) \cdot \text{Arctan}(z/z_R) \qquad (1)$$

for the TEM_{mn} transverse mode, where z_R is the Rayleigh length of the hermite gaussian beam. This then gives us the ability to determine the origin of each misalignment. A TEM_{01} signal that has traveled from the input mirror to the end mirror and back will have a different phase shift as compared to a TEM_{01} that has only traveled from the end mirror.

Using Guoy phase telescopes, we can demodulate with different Guoy phases and thus isolate different alignment signals.

The setup for LIGO II is much more complicated than a Fabry-Perot cavity, however, and takes more work to keep in alignment. The primary complication is the increased number of mirrors in the system. Where a Fabry-Perot cavity has only two mirrors that can be misaligned, the signal-recycling LIGO II Dual-Recycled Michelson Interferometer has 6 that are essential for maintaining a high signal-to-noise ratio. These include the 4 in each arm that construct the Fabry-Perot cavities, one power recycling mirror that resides between the input laser and the beam splitter, and one signal recycling mirror at the dark port. Also, instead of just one sampling of the laser to form an error signal, in the LIGO II configuration there are three samplings of the laser at different places in the interferometer. There is a detector at the reflected port, just like a Fabry-Perot cavity, plus there is one at the dark port past the signal recycling mirror, and there is a pick off between the beam-splitter and one input test mass. Also new is a subcarrier frequency added in the beam, along with the normal sidebands, to help control the signal recycling mirror and it introduces a whole host of new demodulation frequencies. A diagram outlining the proposed setup for the signal recycled interferometer is given below in fig. 3.

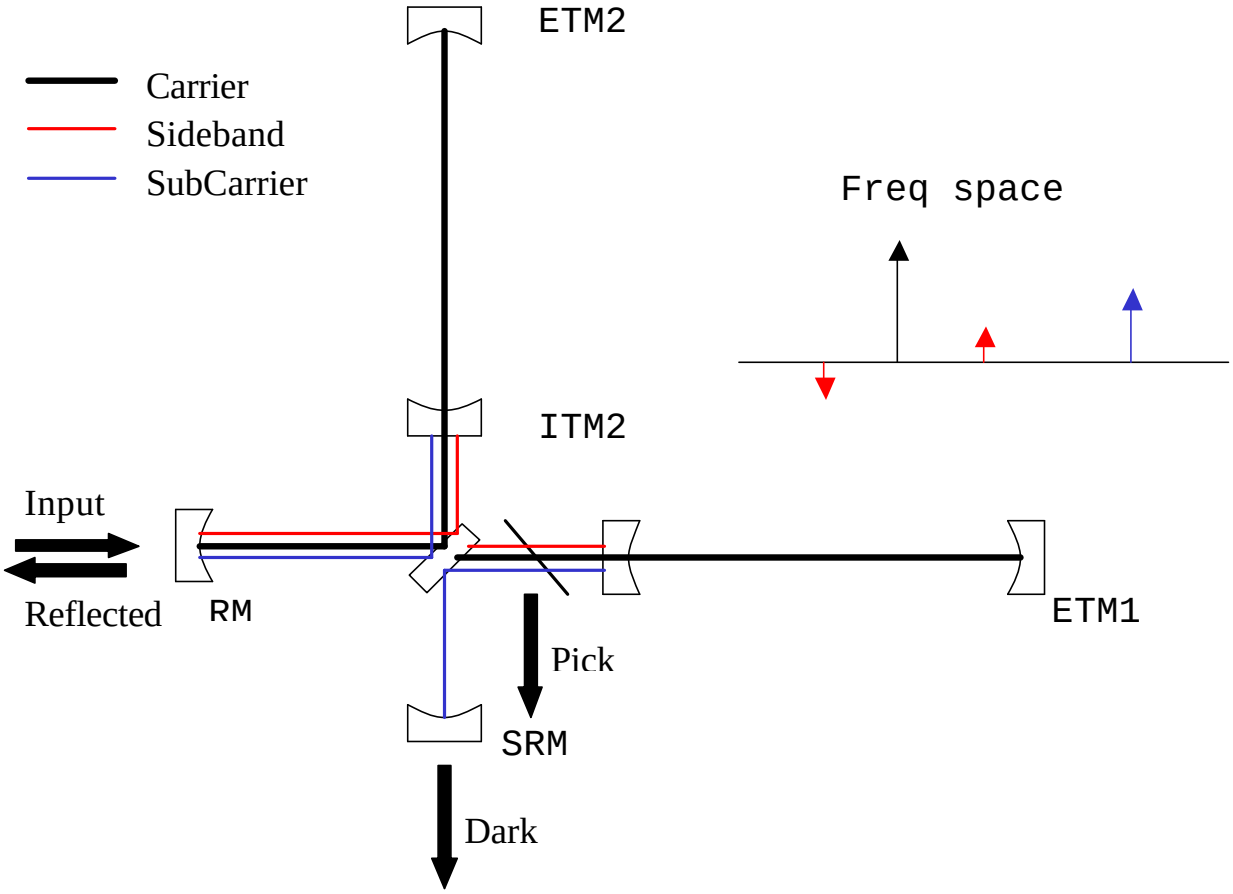

Fig 3. Resonance scheme proposed for signal recycling.

With the resonance setup shown in fig 3, we can control the mirrors by looking at the output at three different ports: the reflected, dark, and pickoff. In a very general sense, the RF sidebands are used in controlling the recycling cavity and arms, while the subcarrier is used to control the signal recycling mirror.

In order to develop an error signal, we need to model what signals we would expect to see based on a given misalignment. Daniel Sigg and Nergis Malvalvala have

developed a Mathematica package called Modal Model, which models an ideal, but misaligned, interferometer and any internal fields. With this package, we can extract what signals we should see if any mirror is misaligned a given amount.

The parameters used for the 40m interferometer in my calculations are as follows:

```
GLOBAL CONSTANTS
****************
laser wave length    :  l = 1064 nm
Refractive index     :  n = 1.44968

ARM CAVITY CONSTANTS
********************
Cavity length        : A1 = 38.8154 m
                       A2 = 38.8154 m
Curvature ETM        : A1 = 61 m
                       A2 = 61 m
Curvature ITM        : A1 = ¥ m
                       A2 = ¥ m
Power refl. ETM      : A1 = 99.9965 %
                       A2 = 99.9965 %
Power trans. ETM     : A1 = 0.0015 %
                       A2 = 0.0015 %
Power refl. ITM      : A1 = 96.998 %
                       A2 = 96.998 %
Power trans. ITM     : A1 = 3. %
                       A2 = 3. %

ARM CAVITY PARAMETERS
*********************
Cavity power refl.   : A1 = 0.992783
                       A2 = 0.992783
Waist Size           : A1 = 3.15253 mm
                       A2 = 3.15253 mm
Rayleigh range       : A1 = 29.3446 m
                       A2 = 29.3446 m
Guoy phase           : A1 = 52.9106 °
                       A2 = 52.9106 °
Spot size ETM        : A1 = 5.22756 mm
                       A2 = 5.22756 mm
Spot size ITM        : A1 = 3.15253 mm
                       A2 = 3.15253 mm
Finesse              : A1 = 205.904
                       A2 = 205.904
Divergence angle     : A  = 107.432 urad

RECYCLING CAVITY CONSTANTS
```

```
*************************
Cavity length         :  C = 2.04292 m
                         A = 2.72388 m
                         D = 0.151119 m
Curvature             : RM = -260 m
                       DRM = -262 m
Power refl.           : RM = 79.998 %
                        BS = 49.9625 %
                       DRM = 79.998 %
Power trans.          : RM = 20. %
                        BS = 49.9625 %
                       DRM = 20. %

ITM curvature in RC     A1 = ¥ m
                        A2 = ¥ m

Matched cuvature      : RM = -423.55 m
                       DRM = -318.855 m


RECYCLING CAVITY PARAMETERS
***************************
Waist Size            : RC = 3.15253 mm
                       SRC = 3.15253 mm
Rayleigh range        : RC = 29.3446 m
                       SRC = 29.3446 m
Guoy phase            : RC = 3.9824 °
                       SRC = 5.30323 °
Spot size             : RM = 3.16016 mm
                       DRM = 3.16609 mm
Max. finesse          : RC = 28.1398
                       SRC = 28.1398

RM curvature at inp.    RC = -292.168 m


MODULATION FREQUENCIES
**********************
FSR                     A1 = 3861.77 kHz
                        A2 = 3861.77 kHz
                        RC = 73.3737 MHz
Sideband frequency      SB = 36.6868 MHz
SubCarrier freq         SC = 110.06  MHz
Modulation depth        SB = 0.5
```

The Modal Model package uses classical wave propagation techniques to model the fields in the interferometer. In order to solve for the effects of a misaligned mirror, we define a normalized angle:

$$\Theta_x = \theta_x \, w(z)/\lambda \qquad (1)$$

where w(z) is the waist size at the optic, θ_x is the misaligned angle given in radians and λ is the wavelength of the laser. A significant displacement of the normalized angle introduces a specific (calculable) amount of TEM_{01}.

Modal Model can introduce a misalignment to any mirror in the system, and simulate the effect on any field of the interferometer. We do not, however, move each mirror individually and see its effect, but rather move groups of mirrors. The math of a Michelson interferometer lends itself to symmetric or antisymmetric movement. To explain the reasoning for this it is easier to think of a simple Michelson interferometer with a single mirror at each arm. If we tune the Michelson to where one of the ports is completely dark, in perfect alignment, all light will come out of the other now "bright" port. In this situation (as is LIGO's), the interferometer is sensitive to 2 degrees of freedom, one where the length of one arm changes without the other (causing light to leak out the dark port) and one where the two arm lengths change lengths at the same time (causing a phase shift at the bright port, but nothing else). In the same way signals in the LIGO interferometer are more easily thought of in "common" and differential modes. Graphical representations of the degrees of freedom are given in Fig 4.

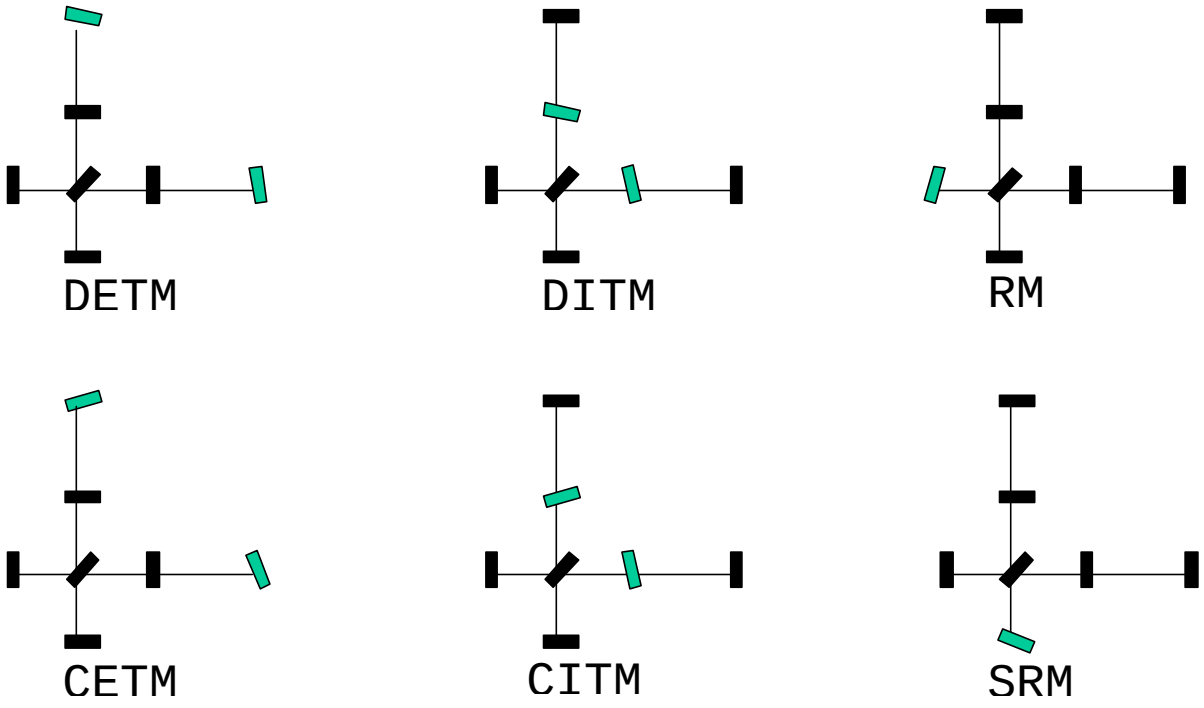

Fig 4. Degrees of Freedom

Modal Model calculates the effects of an angular misalignment of each of the 6 DOFs defined above on the carrier and sideband light exiting each of the three ports (dark, bright and pickoff, given in Fig 3). The code simulates the response of a split photodiode to TEM01 (pitch) or TEM10 (yaw) light, with zero response for TEM00 mode light. It then simulates the procedure of mixing the photodiode signal with the reference RF source used to generate the sideband light at the input port. The result is a signal whose amplitude is a measure of the misalignment of each of the 6 DOFs, along with the RF phase which maximizes this signal, and the Guoy phase advance from the misaligned element to the output port. The Guoy phase denotes how the higher order

modes have shifted with respect to the RF.

	DETM	DITM	CETM	CITM	RM	SRM
Dark - Cr-SB	-1.84566	-0.666123	0.00080783	0.000291557	-0.00611958	-9.98756×10^{-16}
RF Phase	152.9	152.9	152.9	152.9	152.9	104.6
Guoy Phase	89.7	89.9	48.2	48.3	89.5	93.9
Bright - Cr-SB	0.157339	-7.42251	-3.75393	-20.1029	23.987	1.41319
RF Phase	143.1	143.3	133.9	148.9	150.9	139.5
Guoy Phase	125.8	126.5	86.5	124.2	126.9	125.6
Pick - Cr-SB	1.54802	-73.0236	-34.4153	-197.855	238.406	13.9031
RF Phase	143.3	143.3	158.6	150.2	149.5	139.5
Guoy Phase	125.8	126.5	85.7	124.5	126.8	125.6
Dark - SB-SC	0.025871	-1.22616	0.0472952	-2.24155	2.73872	-0.27049
RF Phase	21.8	21.8	0.6	0.6	3.5	140.
Guoy Phase	132.9	132.9	41.5	41.5	31.6	104.
Bright - SB-SC	-0.0788971	3.73938	-0.249326	11.8169	-14.7598	1.08385
RF Phase	132.5	132.5	167.8	167.8	166.3	3.6
Guoy Phase	12.9	12.9	54.9	54.9	56.8	59.2
Pick - SB-SC	-0.917404	43.4809	-3.20855	152.07	-174.458	13.9161
RF Phase	149.6	149.6	170.9	170.9	169.4	0.5
Guoy Phase	12.8	12.8	39.9	39.9	34.3	39.5
Dark - Cr-SC	-4.89869×10^{-6}	7.31341×10^{-6}	-1.09831×10^{-8}	1.14711×10^{-8}	-1.673×10^{-6}	9.53968×10^{-16}
RF Phase	136.4	46.3	44.	142.6	152.2	31.
Guoy Phase	46.2	136.2	92.2	11.	61.7	129.3
Bright - Cr-SC	-0.00877758	-0.0363025	-1.62343	6.71421	-2.68049	0.
RF Phase	9.8	99.7	107.2	17.1	33.6	0
Guoy Phase	66.5	156.6	17.	107.1	91.5	0
Pick - Cr-SC	-0.0910084	-0.376395	-16.8321	69.6148	95.3959	0.
RF Phase	9.8	99.8	107.2	17.1	151.4	0
Guoy Phase	66.5	156.6	17.	107.1	147.5	0

Table 1. Modal Model Output -- On the left denotes the output port and at what demodulation each signal is from. The signal is in units of incident watts per normalized degree angle change.

In order to develop an error signal for each degree of freedom (DOF), we need to figure out a port and a demodulation where that degree of freedom has a strong signal and all others do not. This amounts to generating a matrix, call it a wavefront sensing matrix, where each row is a specific port and demodulation (with phases). The goal is to make this matrix as diagonal as possible, thus minimizing the cross-coupling between each DOF. In each row, we choose RF and Guoy phases which make the response to most or all DOF's close to zero except for one, which dominates. This produces a more diagonal control matrix. The signal is then given by equation 2:

$$WFS = Ampl\ Cos(RF_0 - RF)\ Cos(Guoy_0 - Guoy) \qquad (2)$$

Where we are able to choose RF_0 and $Guoy_0$ using Guoy phase telescopes and standard demodulation techniques.

Results

One of the first trials I did with Modal Model was to attempt to duplicate other published results. Specifically, I wanted to duplicate the signals for a LIGO I setup (no signal recycling mirror) given in a paper by Nergis Malvalvala and Daniel Sigg[1]. The results I obtained are in table 4, below.

	DETM	DITM	CETM	CITM	RM
Dark - Cr-SB	-24.9815	-11.3941	-9.89027×10^{-6}	-4.51095×10^{-6}	-0.00122482
RF Phase	90.	90.	90.	90.	90.
Guoy Phase	90.2	90.5	156.2	156.5	90.2
Bright - Cr-SB	0.0228234	-1.36698	-0.725762	6.20788	-9.60156
RF Phase	90.1	90.	0.	0.	0.
Guoy Phase	143.7	143.7	96.8	145.9	146.5
Pick - Cr-SB	6.13013	-367.157	47.7087	1730.26	-2401.56
RF Phase	90.	90.	0.	0.	0.
Guoy Phase	143.7	143.7	61.1	143.	143.7

Table 4. LIGO I configuration results for 4km parameters

These results are in excellent agreement with those reported in ref 1, tables 2 and 3. This gave me sufficient confidence to trust the numbers that I then calculated for the LIGO II setup.

Using the above Modal Model output (table 1), I was able to derive the following wavefront sensing matrix:

DETM	**DITM**	**CETM**	**CITM**	**RM**	**SM**
-1.84563	-0.666122	0.000602218	0.000217688	-0.00611935	0
0.122136	-5.78869	0	0	0	0.210337
0.000471355	0.0326537	-1.56438	0	0	0
-0.0429213	-0.191573	0.0204811	49.8228	0	0
0.00879329	-0.241971	0	0	51.9161	0
0	0	-0.00294052	0.139366	0	-0.227225

Table 2. WFS matrix scheme for 40m

The columns are the same as in table 1 and the rows are as follows:

1: Dark -- Cr - SB RF: 152.9 Guoy: 90
2: Pick -- SB - SC RF: 80.9 Guoy: 124.3
3: Bright -- Cr - SC RF: 107.1 Guoy: 1.5
4: Pick - Cr - SC RF:61.4 Guoy: 107.1
5: Pick - Cr - SC RF: 107.1 Guoy: 107
6: Dark -- SB - SC RF: 111.8 Guoy: 121.6

Table 3. Rows of the WFS matrix

I was pleased at how diagonal I was able to make the matrix. Overall, there are only two wavefront sensors that yield coupled signals.

Discussion

Although I say that I trust my results, I can't say that I was incredibly encouraged by them. Where in LIGO I, most of the disturbances yielded nice RF phase shifts and had predictable grouping of guoy phase shifts. In other words, you could predict which ports would be sensitive to which disturbances and what groups of disturbances would yield the same phase shifts. In the LIGO II situation, everything changed. Nothing was predictable, and many things were unexpected. I was able to pick out a control scheme, however, but it was significantly different from LIGO I, which made me uneasy. Yet, after a week of looking at the results, I am starting to see some of the reasons for the strange phases and signals and have become more confident.

For completeness, I decided include the rational for my row choices for the alignment sensing scheme found in table 2.

Row by row:

1: This port had the largest relative DETM signal, RF and Guoy chosen to maximize signal from DETM and DITM and minimize the signal from the other 4 DOFs.

2: This port had a relatively large DITM signal, but more importantly, had its rf and guoy phases significantly seperated from CITM and RM. The RF phase was chosen to eliminate response to the CITM DOF, and the Guoy phase was chosen to eliminate response to the RM DOF.

3: The control of CETM could also have gone to the pickoff -- Cr - SC, but the bright port has a larger relative signal. Both of these ports exibit the nice properties of having almost no DETM/DITM influence and the two common modes are out of RF phase. The RF phase was chosen to eliminate the response to the CITM DOF, the Guoy phase was chosen to eliminate response to the RM DOF.

4: Same reasoning as 3, only the pickoff favored CITM. The RF phase was chosen to eliminate response to the RM DOF, and the Guoy phase was chosen to eliminate response to the CETM DOF.

5: This was the only port where RM did not have almost the exact RF and Guoy phase as CITM. The RF phase was chosen to eliminate response to the CITM DOF, The Guoy chosen to eliminate response to the CETM DOF.

6: This was the best port for controlling the SRM for one reason: it was the only SRM signal with RF and guoy phases significantly seperated from all other signals. And RM had a guoy phase very close to CITM/CETM which helped reduce all of the signals; Pick -- SB - SC is another option for this WFS but doesn't have quite as good guoy phase agreement between RM and CITM/CETM. The RF phase was chosen to eliminate response to the DETM/DITM DOFs, and the Guoy phase was chosen to eliminate response to the RM DOF and reduce response to the CITM DOF.

Conclusions

Modal Model was used to calculate alignment signals for the 40m LIGO Prototype and for a proposed version of LIGO II, with a signal recycling mirror. I have confidence in my results because I was able to duplicate previously generated results for the simpler LIGO I configuration. The signals seem reasonable, and from them I was able to compose an extremely diagonal alignment sensing scheme.

Acknowledgements

First I'd like to thank my mentor Alan Weinstein for helping me through the project and for all the encouragement. Nergis Malvalvala and Daniel Sigg designed Modal Model and helped me when I had difficulty. Dennis Ugolini and Steve Vass were a continual source of information around the lab. And last, I'd like to thank Ken Libbrecht and the entire LIGO program for making all of this possible.

Bibliography

Signal Extraction and Control for an Interferometirc Gravitational Wave Detector by Martin W Regehr. – 1995

Alignment Issues in Laser Interferometric Gravitational-Wave Detectors by Nergis Mavalvala – Jan 1997

Principles of Calculating Alignment Signals in Complex Resonant Optical Interferometers by Yaron Hefetz, Nergis Mavalvala, Daniel Sigg – Nov. 1996

[1]*Alignment of an Interferometric Gravitational Wave Detector* by P. Fritschel, G. Gonzalez, N. Mavalvala, D. Shoemaker, D. Sigg, and M. Zucker – April 1998

Principles of calculating the dynamical response of misaligned complex resonant optical interferometers by Daniel Sigg and Nergis Mavalvala – Sept. 1999